



ÉCOLE POLYTECHNIQUE
FÉDÉRALE DE LAUSANNE

**Energy management strategies for reducing a
building's electricity costs after a PV installation**

Semester project report - LCA

Pol Boudou Pérez

Autumn 2020

Supervisor: Dr. Jagdish Prasad Achara

Laboratory for Communications and Applications LCA
Prof. Jean-Yves Le Boudec

Contents

1	Introduction	3
2	Context	4
2.1	Baseline scenario	4
2.2	Assumptions	6
2.3	Preliminary notations	6
3	Control strategies	7
3.1	Strategy 1: rule-based control of boilers for self-consumption	7
3.2	Strategy 2: adding a battery to enhance self-consumption	11
3.3	Strategy 3: MPC of boilers for cost optimization	15
3.4	Strategy 4: MPC of battery and boilers for cost optimization	17
4	Implementation and Simulation conditions	19
4.1	Software architecture	19
4.2	Building case and simulation characteristics	20
5	Results	24
6	Discussion	30
6.1	Battery integration: a questionable option	30
6.2	MPC: confirmed benefits and limitations	30
6.3	Study limitations	30
7	Conclusion	32
A	Linearization of MPC formulation	33

1 Introduction

The number of photovoltaic (PV) installations have increased exponentially over the last decades and the trend is expected to continue [4]. On top of falling prices of PV modules, this trend has been driven by policy and regulatory measures. One example is the Feed-in Tariff (FiT), a well-established policy scheme introduced to incentivize the adoption of renewable technologies consisting in paying owners a fixed price for the energy they inject into the grid [1].

Since well-built solar PV systems last 30 years or more, regulatory programs like the FiT have made the installation of PV systems largely profitable in many countries. As time goes by, some have even found themselves over-paying PV owners [2]. On top of that, the increasing penetration of distributed PV generation poses technical challenges to the operation of distribution grids. This is especially the case in Medium Voltage (MV) and Low Voltage (LV) networks, which are more vulnerable to the intermittency of PV production. Problems such as reverse power flow, voltage variation, or feeder congestion are well known and can be found in the literature [5].

Mainly for those two reasons (increased profitability and technical limitations), incentives for PV installations are now taking an opposite trend. European countries are lowering their Feed-in tariff programs at a faster pace, and some like the UK have even closed the scheme [6].

On one side, solar installations are getting cheaper, but on the other, a proper and profitable integration is challenged by a less favorable electricity pricing structure. As a result, it is becoming necessary for PV owners to support such installations with Energy Management Systems (EMS).

As PV generated electricity is "free" (i.e. already paid) for the adopter, the reduction of electricity bills can simply come from self-consumption. The randomness and non-controllability of PV power reverses roles, forcing demand to be flexible and reactive to supply. This can be the role of an EMS, which monitors and controls power demand in order to improve the performance of the electrical system, and for example, reduce associated costs or emissions. In a building, the more flexible loads are available to be controlled, the more the potential for an EMS to shift demand so it matches solar supply.

Energy management is performed by connecting through a communication network the different flexible loads to a central controller, which ruled by a control algorithm will set the right command for each of the loads. Control algorithms can take different levels of complexity, going from a myopic rule-based logic, unable to anticipate any future behaviour, to model predictive control, where the introduction of forecasts give the EMS a far-sighted view and the ability to optimize upon that building's consumption. Ultimately, the selection of an appropriate approach as well as the design of the algorithm will be carried according to the building characteristics, and also the grid's.

This report addresses the case of a standard residential building equipped with a PV system, electric boilers, and casual domestic loads. It first proposes various ways or strategies for reducing the electricity bill of the building by designing an appropriate Energy Management System. The control algorithms as well as the tools and systems needed for implementing each of the EMS are mentioned, pointing the advantages and disadvantages of each. Through the study, an emphasis is given on the distinction between myopic and prediction-assisted control approaches. Also, the economical benefits of installing an energy storage battery as additional flexibility for the EMS are analyzed. In order to draw conclusions regarding the performance of each of the energy management strategies,

a specific study case is defined and simulated.

All in all, through the simulation of concrete study case, this report is intended to give insights about some of the practices to reduce a building's electricity bill. First, the five different strategies are accurately described. Second, the simulation framework is presented, as well as the specific conditions used to draw the cost analysis. Then, results are presented, showing a progressive cost reduction over the five compared strategies. In the end, after analyzing results, the relevant limitations of the study are discussed.

2 Context

2.1 Baseline scenario

The baseline scenario describes the case of a modern residential building. It hosts several households and has a central power connection point where all domestic appliances power consumption is summed up in order to connect to the grid. For heating, the building is equipped with two electric boilers that act as central sources of hot water.

When households consume hot water, such volume is drained from the two boilers, which reduces their temperature. For that reason, their temperature needs to be monitored and subsequently controlled to stay at the desired level, called $\underline{T}_{B,k}$. Boilers are controlled by a simple hysteresis type controller that keeps their temperature in a short range around their desired state. Whenever their temperature declines below that level, boilers are powered at their rated power until a certain new temperature $\underline{T}_{B,k} + T_{\Delta}$ is measured. The threshold T_{Δ} can typically be around 0.5 °C, and simply ensures that boilers do not switch too fast between ON and OFF power modes.

The control logic as well as the necessary tools to make it function are integrated locally at each boiler. Those are equipped with a sensor able to communicate data to an embedded system, which computes the adequate control and send it to an actuator which enforces such command.

In order to produce locally and reduce the building's electricity bill, a PV system has recently been incorporated on the rooftop. Now that the building can not only consume power but also generate it, it can be seen as a grid-connected microgrid (see Figure 1). In fact, it can inject excess PV power into the grid via a single two-ways connection. When solar power is not enough to supply the building's different loads, power will be demanded from the grid, just like before the PV installation.

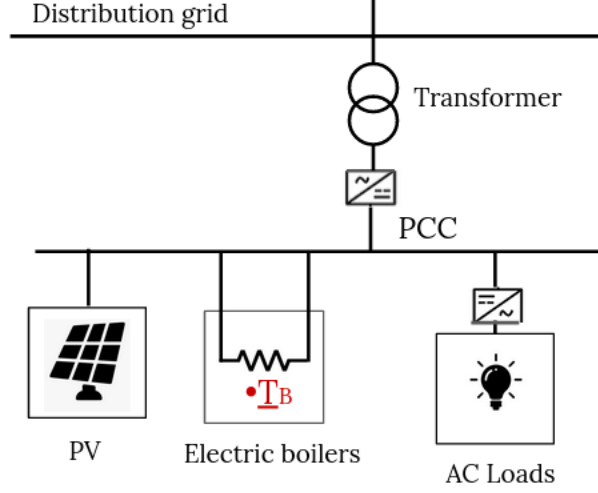


Figure 1: Building's electrical system can be seen as a grid-connected microgrid. The power supplied by the PV system and demanded by controllable boilers and non-controllable loads sum up at the Point of Connection Coupling (PCC). Boiler's temperatures are controlled to stay around $T_{min} = \underline{T}_{B,k}$

Regarding the pricing structure, the building in the baseline scenario can be subjected to a variety of electricity rates. For instance, the feed-in tariff (FiT) that the household gets for injecting power back to the grid is constant and considerably lower than the price it pays to the grid for consuming electricity. This FiT often depends on the size of the PV, the time of installation and the geographical area. On the other side, the buying price can be constant but also variable, taking several time-based pricing options such as time-of-use pricing (TOU), critical-peak pricing (CTP) or even real-time pricing (RTP) (see Figure 2).

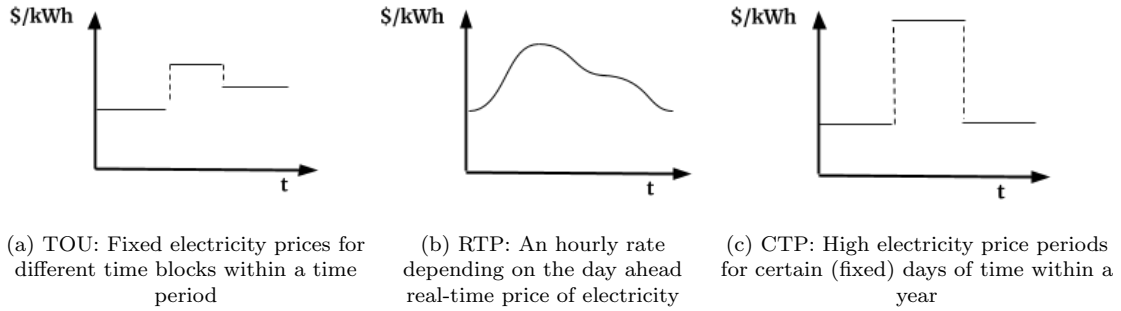


Figure 2: Basic time-based pricing options [3]

The pricing structure in this scenario is left without further specifications as in reality, it can largely depend on the settlement with the grid operator. Furthermore, assuming a progressive liberalization of the electricity market, those price patterns could be set 24 hours in advance and be highly influenced by the region's power supply and demand.

2.2 Assumptions

In this study, the primary quick control ensuring correct real-time load sharing is taken for granted. Usually in the millisecond range, a distributed control at the load level ensures local protection of the building's electrical system. The strategies presented in this report will be based on top of that layer, as a secondary slower control performing energy management.

As presented in Figure 1, it is also assumed that the PV converter is connected to the building's electrical system and not to the distribution grid directly. The central power connection point regroups therefore all of the building's loads as well as PV power. It is therefore assumed that the PV installation respects building power limits, which will not be surpassed even at peak production.

Under such assumptions, it is important to precise that the building's primary control automatically balances power supply and demand. Any PV power not consumed by the building is absorbed by the grid without the necessity of any secondary control action set by an EMS. Similarly, any power demand from loads that cannot be supplied by the PV system is automatically supplied by the grid.

2.3 Preliminary notations

In order to present the energy state of the building as well as the boilers temperature being controlled, the relevant variables of this scenario need to be defined.

Time index of the variables is noted with $[h]$, where h designates the current discrete time period of length Δt . Regarding sign convention, a power is positive if it is injected into the microgrid (for instance by the PV system) and negative if absorbed by loads. Underline ($\underline{\bullet}$) and overline ($\overline{\bullet}$) designate minimum and maximum values respectively. Finally, bold variables designate vectors, usually regrouping the states of the two boilers. Indexes refer to specific energy systems.

Electric boilers

$u_{B,k}$: target power set by controller for boiler k (kW) (≤ 0)

$p_{B,k}$: actual power of boiler k (kW) (≤ 0)

$\overline{P}_{B,k}$: Rated power of boiler k (kW) (≤ 0)

$T_{B,k}$: actual temperature of boiler k ($^{\circ}\text{C}$)

$\underline{T}_{B,k}$: desired minimum temperature of boiler k ($^{\circ}\text{C}$)

$T_{\Delta,k}$: hysteresis threshold of boiler k ($^{\circ}\text{C}$)

$E_{B,k}$: energy (heat) demanded to boiler k (kWh)

Vectors \mathbf{T}_B , $\mathbf{p}_{B,k}$ \mathbf{u}_B regroup information of both boilers.

Microgrid power state

p_{PCC} : PCC power (kW) (positive when PV supply $>$ load demand, else negative)

Grid's buy and sell rates

$C_{buy}[h]$: electricity buying rate (CHF/kWh) (> 0)

$C_{sell}[h]$: electricity selling rate (CHF/kWh) (≥ 0)

3 Control strategies

3.1 Strategy 1: rule-based control of boilers for self-consumption

Because controllable loads bring a degree of freedom to the building's energy state, the implementation of an EMS can translate into cost reductions. In the present case, two boilers are the unique controllable loads, and an EMS is designed to exploit the energy flexibility they bring to the building. In some sort, although their output is heat and not power, boilers B1 and B2 can be seen as thermal storage. If PV production is freely available in the building and non-controllable loads are not consuming all of it, this power can be used to "charge" boilers instead of feeding the grid.

The first energy management strategy consists in operating those thermo-electric units under certain coordination to actively respond to the building's power fluctuations brought by non-controllable loads and PV generation.

For that, an acceptable upper temperature limit $\overline{T}_{B,k}$ is set for each boiler k . Their temperature will not stay anymore around their desired temperature $\underline{T}_{B,k}$ but will be let flexible to take higher values with the goal to "store" energy given by PV surplus. Those two temperature ranges for boilers B1 and B2 will constitute the only degree of freedom for the EMS to operate. Now, in contrast to the supply side which is non-controllable, the demand side will be controlled with the goal of matching solar production.

EMS Components and boiler modelling for control

As described in the baseline scenario (see section 2.1), it is assumed that the different loads are self-conscious about their state. Boilers are equipped with temperature and power sensors. The household power consumption as well as the PV power generation are measured at the point of common coupling (PCC), therefore as a single measure.

The new EMS implementation requires a central controller able to interpret all of these measurements. An additional communication layer is deployed to centralize the load measurements and allow the controller to compute actions that enhance the overall energy and power state of the building. The central controller of strategy 1 is designed to receive and handle the 5 physical quantities measured by sensors:

- Power at PCC
- Power being supplied to Boiler 1
- Power being supplied to Boiler 2
- Temperature of Boiler 1
- Temperature of Boiler 2

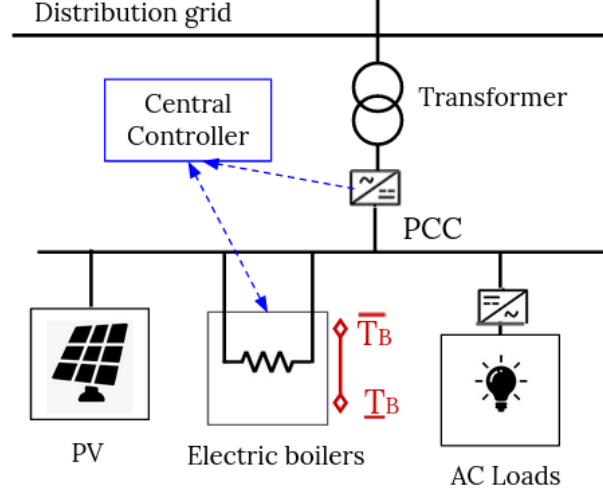


Figure 3: Electrical system of the microgrid, where an EMS composed of a central controller and a communication layer (blue) is added. Controller receives the power state of the microgrid as well as boilers' power and temperatures. Taking advantage of the temperature flexibility brought by boilers (red), the controller can set their actions in order to enhance self-consumption.

The different sensors broadcast their measurements with a certain period, typically of tens of seconds. With a similar or lower frequency, the controller processes such inputs and computes an adequate control action for each of the controllable units. The output is communicated back to the loads, where the actuator ensures that the controller orders are executed.

In order to actively control the two boilers, their functioning has to be somehow modelled. The controller commands cannot be given to a boiler without knowing which impact will they have on boiler's temperature. With the use of a model, the controller can estimate how these entities will evolve as a function of the commanded power and hence allow an adequate supply. For strategy 1, a relatively simple and linear model is used. The boiler's heat capacity C_B describes its ability to accumulate heat. Ignoring factors such as heat loss, hot-water consumption and electrical efficiency, the temperature evolution in the boiler is approximated with the difference Equation 1.

$$T_B[h + 1] = T_B[h] - p_B \frac{\Delta t}{C_B} \quad (1)$$

Control algorithm

The controller is configured by establishing rules determined by all possible system operating scenarios. It receives measurements of all system states and uses those to take myopic decisions according to the prescribed rules.

The hysteresis behaviour present in baseline scenario is conserved in order to ensure that a certain minimum temperature is held. Its functioning is illustrated at the beginning of Algorithm 1. Once boiler's lower bound $\underline{T}_{B,k}$ is reached, a binary variable $s_{B,k}$ is set to 1, meaning that the boiler will

be supplied until the new target temperature $\underline{T}_{B,k} + T_{\Delta,k}$ is reached. As long as $s_{B,k}$ remains 1, boiler k will keep being powered at its maximum rated power $\bar{P}_{B,k}$. Once the target temperature is reached, $s_{B,k}$ will be set equal to 0, meaning that the lower limit constraint has been successfully handled. To deal with both boilers, the vector \mathbf{s}_B is defined.

When boilers are not in the critical range defined by $s_{B,k} = 1$, they are exclusively supplied by surplus power. The controller looks at the power state of the building and defines $p_x (= p_{PCC}[h] - (p_{B1}[h] + p_{B2}[h]))$, which represents the available excess power to supply boilers. If such amount is positive and the microgrid has power surplus, some of it (or all) is given to the flexible loads that can take it. In this case, the boiler with the lowest temperature (normalized according to its min and max limits) is considered first, and its control action is computed. If surplus power is still positive, a command for the second boiler will be set.

When powering boiler k , the controller will ideally supply all of the remaining surplus power. However, such a command might be limited by a power or temperature constraint. A lower command may be given considering that the boiler cannot be powered above its rated power $\bar{P}_{B,k}$. Also, boiler power has to be adequate to avoid bringing its temperature above the upper limit $\bar{T}_{B,k}$. To handle that, the boiler's model (c.f Equation 1) allows to compute right amount of power needed to reach $\bar{T}_{B,k}$. More specifically, the controller computes the error between the current and the target temperature ($e_k^T[h] = \bar{T}_{B,k} - T_{B,k}[h]$), which is translated into a power action with the model.

In Algorithm 1, the line $u_{B,k} \leftarrow \max[-C_w \frac{e_k^T[h]}{\Delta t}, \bar{P}_k, -p_x]$ shows how command on boilers will be limited by rather 1) the power needed to attain their desired temperature, 2) their rated power or 3) microgrid's power surplus.

Pseudocode

Algorithm 1 Strategy 1: control of boilers for PV self-consumption

Executed every time-step h

Inputs: $\mathbf{T}_B[h]$, $p_{PCC}[h]$, $p_{B1}[h]$, $p_{B2}[h]$, $\mathbf{s}_B[h-1]$

Control variables: \mathbf{u}_B

Initialize: for all k : **if** $(T_{B,k}[0] < T_{\Delta,k})$: $s_{B,k}[0] = 1$, **else:** $s_{B,k}[0] = 0$

Start

$\mathbf{u}_B \leftarrow 0$

$p_x = p_{PCC}[h] - (p_{B1}[h] + p_{B2}[h])$

sort $\mathbf{T}_B[h]$ in ascending order

for each boiler k **do**

if $T_{B,k}[h] \geq \underline{T}_{B,k} + T_{\Delta,k}$ **then**

$s_{B,k}[h] = 0$

end

if $T_{B,k}[h] \leq \underline{T}_{B,k}$ **then**

$s_{B,k}[h] = 1$

else

$s_{B,k}[h] = s_{B,k}[h-1]$

end

if $s_{B,k}[h] = 1$ **then**

$u_{B,k} \leftarrow \bar{P}_k$

$p_x = p_x + u_{B,k}$

else

if $p_x > 0$ **then**

$e_k^T[h] = \max(0, \bar{T}_{B,k} - T_{B,k}[h])$

$u_{B,k} \leftarrow \max[-C_B \frac{e_k^T[h]}{\Delta t}, \bar{P}_k, -p_x]$

$p_x = p_x + u_{B,k}$

end

end

end

return Control variables

Summary and Limitations

In comparison with baseline scenario, strategy 1 allows to maximize self-consumption, which is supposed to translate into a reduction of the electricity bill. In summary, integrating into the baseline building an EMS capable of implementing strategy 1 requires:

- Knowing boiler specifications (volume, rated power and temperature limits).
- Adding an embedded system serving as a central controller.
- Adding a communication layer for information exchange between controller and loads.

Being the first strategy implemented, the described EMS presents however several limitations. Those are summarized in the following points:

- Inter-interval power variations are not accounted by the controller.
- Very basic modelling of boiler.
- Buildings flexibility is limited by boilers' power and temperature bounds.
- Myopic approach.

First, the controller acts on the measures obtained at time h . It receives those measures and computes the best possible action for time h power state, which may not remain the same during the next time interval of length Δt . In the microgrid, power demand can be perfectly matching supply at the beginning of each control action, but this matching may end once non-controllable power supply or demand varies. For instance, if excess is positive, it is supplied to boilers. A few seconds later, excess could decrease, forcing the main grid to supply some of the power being requested by boilers actuators. This would translate into unnecessary costs.

The second limitation makes reference to the use of a simplistic modelling of boilers. Basically, the model does not account for hot-water consumption and therefore neglects cold water entering the boiler, which is a crucial point when the goal is to control its temperature. Also, outside boiler temperature is not considered and neither are heat losses. Having an incomplete model might give the controller a poor information, and power could be saved by incorporating a model that better describes reality.

Thirdly, capacity limitations might force some of the locally produced power to be re-injected into the grid. If boilers' heat storage capacity is not big enough to absorb all PV power, power would be re-injected into the grid, which depending on the pricing structure could represent an economic disadvantage.

Last but not least, the algorithm is rule-based and myopic, meaning that it acts based on the set of measurements available at the present time. Because of that, it cannot take into consideration the variable prices of electricity grid. This impedes the EMS to get the most out of the flexibility of boilers, that could be supplied plentifully when grid's electricity is cheaper and avoid doing it when it is expensive. By incorporating predictions of future behaviour of the different energy units, the EMS would be able to anticipate variations in supply and demand and manage resources more effectively in order to reduce the overall electricity bill.

3.2 Strategy 2: adding a battery to enhance self-consumption

Strategy 1 proposed the base layer to profit from the building's PV installation. By adapting demand to supply, self-consumption could be enhanced and power demanded from the grid reduced. However, at moments when boilers are fully powered or at maximum temperature, some excess power may be re-injected into the grid at a lower price. In those cases, flexibility brought by boilers will not be enough to make the most out of the PV production.

One solution to further maximise self-consumption is to install into the building an energy storage battery system. This will add a level of flexibility to the EMS and will be able to shape the power system fluctuations by both consuming and producing power when desired.

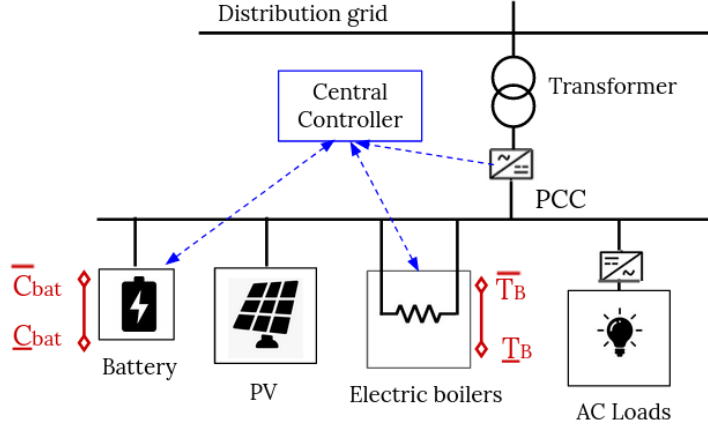


Figure 4: Electrical system and communication network (blue) needed for strategy 2, where a battery is incorporated to add a new degree of flexibility (red).

Because the battery is only going to step in after the flexible loads have offered their flexibility, a small energy storage device is sufficient. In fact, it is not needed to store all PV power, but rather to bring to the microgrid a little extra self-consumption ability. Moreover, putting the battery last in the power supply priority is going to reduce pointless charge/discharge cycles, which are the main source of battery deterioration and aging.

EMS Components and battery modelling for control

On top of the EMS architecture required for strategy 1, the incorporation of the battery adds some complexity to the building energy system. A new control variable needs to be taken into account, and a battery model (Equation 2) is needed for the controller to determine an adequate control action.

$$x_{bat}[h+1] = x_{bat}[h] - p_{bat}[h] \Delta t \quad (2)$$

$$\underline{C}_{bat} \leq x_{bat}[h] \leq \overline{C}_{bat} \quad (3)$$

$$\overline{P}_{bat}^{ch} \leq p_{bat}[h] \leq \overline{P}_{bat}^{disch} \quad (4)$$

The battery's State-of-Charge x_{bat} (kWh) and power p_{bat} (kW) are now measured and broadcasted to the controller. Capacity limits are described by Equation 3, where \overline{C}_{bat} and \underline{C}_{bat} are respectively the maximum and minimum battery capacity (kWh). Regarding power limits in Equation 4, \overline{P}_{bat}^{ch} (≤ 0) and $\overline{P}_{bat}^{disch}$ (≥ 0) are respectively the maximum charging power and maximum discharging power (kW). In this model, charging and discharging efficiencies are assumed to be 100% and no

leakage phenomenon is considered.

The constraints are known by the controller, which will set the correct battery power u_{bat} to keep the device within its limits. On top of that, the Battery Management System (BMS) incorporated within the storage device ensures its secure operation, stepping in if the controller command is slightly inadequate.

Control algorithm

Like in previous strategy, the controller's algorithm looks at boilers states to supply them if they are below their lower temperature limits. Once this specific case is handled, surplus power is given to boilers first and battery second. In the case of a negative power at PCC, the system has now an alternative to cover the demand: the battery is discharged accordingly and provided that such demand lies within its capacity and power limits (Equations 3 and 4 respectively). When this is not the case, the remaining demand is absorbed from the main grid. Algorithm 2 presents the control logic implemented in strategy 2.

Algorithm 2 Strategy 2: control of boilers and battery for PV self-consumption

Executed every time-step h

Inputs: $\mathbf{T}_B[h], p_{PPC}[h], p_{B1}[h], p_{B2}[h], \mathbf{s}_B[h-1], p_{bat}[h], x_{bat}[h]$

Control variables: \mathbf{u}_B, u_{bat}

Initialize: for all k : **if** $(T_{B,k}[0] < \underline{T}_{B,k} + T_{\Delta,k})$: $s_{B,k}[0] = 1$, **else**: $s_{B,k}[0] = 0$

Start

$p_x = p_{PPC}[h] - (p_{B1}[h] + p_{B2}[h] + p_{bat}[h])$

sort $\mathbf{T}_B[h]$ in ascending order

for each boiler k **do**

if $T_{B,k}[h] \geq \underline{T}_{B,k} + T_{\Delta,k}$ **then**

$s_{B,k}[h] = 0$

end

if $T_{B,k}[h] \leq \underline{T}_{B,k}$ **then**

$s_{B,k}[h] = 1$

else

$s_{B,k}[h] = s_{B,k}[h-1]$

end

if $s_{B,k}[h] = 1$ **then**

$u_{B,k} \leftarrow \bar{P}_{B,k}$

$p_x = p_x - p_{B,k}[h] + u_{B,k}$

end

if $p_x \geq 0$ **and** $s_{B,k}[h] = 0$ **then**

$e_k[h] = \max[0, (\bar{T}_{B,k} - T_{B,k})]$

$u_{B,k} \leftarrow \max[-C_B \frac{e_k[h]}{\Delta t}, \bar{P}_{B,k}, -p_x]$

$p_x = p_x + u_{B,k}$

end

end

if $p_x \geq 0$ **then**

$u_{bat} \leftarrow \max[\frac{x_{bat}[h] - \bar{C}_{bat}}{\Delta t}, \bar{P}_{bat}^{ch}, -p_x]$ (charge battery)

else

$u_{bat} \leftarrow \min[\frac{x_{bat}[h] - \underline{C}_{bat}}{\Delta t}, \bar{P}_{bat}^{disch}, -p_x]$ (discharge battery)

end

return Control variables

End

Limitations

The incorporation of a battery system does not add any particular implementation difficulty to the EMS of previous strategy. Such integration is however backed by a poor representation of the battery's state evolution. Parameters such as charging and discharging efficiencies as well as battery leakage coefficient are not considered. By studying the battery specifications and properly updating controller's logic with an accurate model, a more precise control action could enhance battery usage.

3.3 Strategy 3: MPC of boilers for cost optimization

Previous strategies were myopic, solely basing their control actions on the last measured states of the energy system. The inability to see into the future made the EMS incapable of taking into account the variability of electricity prices.

By estimating with some advance the daily power needs of the building, controllable loads can be scheduled appropriately to reduce the overall electricity bill. As presented in the initial assumptions, this electricity price $C_{buy}[h]$ can be variable and is known 24 hours in advance. Similarly, the price $C_{sell}[h]$ set by the grid to buy building's surplus is usually constant.

By forecasting the uncontrollable variables that have an impact on the building's PCC power, their future state can be taken into account to compute the optimal action for the present moment. On top of electricity tariffs, the introduction of forecasts for PV production, load demand and building's energy usage for hot water will allow the EMS to perform an optimization problem with the goal of minimizing electricity costs.

Because predictions such as the forecasted PV power are subjected to uncertainties, performing a single optimization at time $h = 0$ to determine the whole 24 hours schedule may very well end up not being optimal at all. In fact, the schedule would be based on forecasts that might be far from accurate predictions. To solve that issue, a Model Predictive Control (MPC) approach is taken in this strategy.

In MPC, models of a process as well as future predictions of performance and external variables are used in order to determine controls signals by minimizing an objective function at each step. This optimization problem gives, at each step, a sequence of control actions for the whole horizon H , from which only the first one is implemented. At next time step, the optimization horizon moves away from one period and a new sequence is computed. Model Predictive Control adapts to the uncertainty of the prediction since the implemented action always incorporate the latest observation of the state.

EMS incorporations

On top of forecasting the power state of the building (PV production and power consumption from non-controllable loads), the amount of hot water usage needs to be predicted in order to estimate the temperature evolution of boilers.

A more accurate model for boilers which takes into account the amount of energy $\hat{E}[h]$ drained from them is therefore needed. The model, presented in Equation 5, assumes a constant temperature T_{inc} for the boiler's incoming cold water.

$$T_B[h+1] = T_B[h] - \frac{\Delta t}{C_B} u_B[h] - \frac{E[h]}{C_B} + \frac{E[h] T_{inc}}{C_B} \frac{1}{T_B[h]} \quad (5)$$

The boiler temperature state depends on 1) its present temperature ($T_B[h]$), 2) the temperature increase due to the supplied power ($\frac{\Delta t}{C_B} u_B[h]$), 3) the temperature decrease caused by the energy demanded by the building in terms of hot water ($\frac{E[h]}{C_B}$) and 4) the temperature decrease due to the incoming cold water, whose volume will depend on the energy drained but also on boiler's temperature ($\frac{E[h] T_{inc}}{C_B} \frac{1}{T_B[h]}$).

As boilers' temperature can freely vary between bounds, 1 kWh of heat will not represent the same volume of water at 30 °C than at 50 °C. This introduces a non-linear term in the boiler model. In fact, volume of incoming cold water is equal to volume of drained water, which is intrinsically linked to both heat demand and actual water temperature (Energy \propto Temperature \times Volume). This means that the changes in temperature brought by the incoming water will be inversely proportional to the boiler's temperature.

MPC formulation

The MPC algorithm is an optimization problem intended to minimize the building's electricity price over the time horizon H . The objective function is therefore defined as the cost of electricity bought minus the cost of electricity sold to the grid. The solution will be constrained by 1) the power balance equations such as power flows in the building, 2) the fact that power cannot be supplied and demanded to the grid at the same time and 3) the limitations over boilers' input power. Finally, the boiler's model is added as a constraint so that its temperature can be estimated by the MPC and stay inside the permissible bounds. In the formulation, the symbol $\hat{\bullet}$ above \hat{p}_{PCC} and $\hat{E}_{B,k}$ designate forecasted values.

With the example of the boiler, the iterative MPC process can be illustrated. The estimated energy usage $\hat{E}_{B,k}[h : h + H - 1]$ allows the MPC algorithm to anticipate and compute the next control actions $u_{B,k}[h : h + H - 1]$ that would minimize the cost integrated over the horizon H . This assumes that there will not be errors between reality and predicted values. Then, when the real disturbance $E_{B,k}[h]$ reveals, the model allows the MPC to be aware of boilers next temperature state $T_{B,k}[h + 1]$.

At each control time-step h , the boilers commands are the solutions of the following optimization problem:

$$\begin{aligned}
& \min_{\mathbf{u}_B, \mathbf{T}_B, p_g} \sum_{h=t}^{t+H-1} C_{buy}[h] p_g^+[h] - C_{sell}[h] p_g^-[h] \\
& s.t. \\
& \quad p_g[h] + \hat{p}_x[h] + u_{B1}[h] + u_{B2}[h] = 0 \\
& \quad p_g^-[h] = \max(0, -p_g[h]) \\
& \quad p_g^+[h] = \max(0, +p_g[h]) \\
& \text{for } k = 1, 2 : \\
& \quad T_{B,k}[h + 1] = T_{B,k}[h] - A u_{B,k}[h] + B \frac{\hat{E}_{B,k}[h]}{T_{B,k}[h]} - C \hat{E}_{B,k}[h] \\
& \quad \bar{P}_{B,k} \leq u_{B,k}[h] \leq 0 \\
& \quad \underline{T}_{B,k} \leq T_{B,k}[h] \leq \bar{T}_{B,k}
\end{aligned}$$

p_g stands for power supplied to or demanded from the grid. When power is supplied to the building, p_g is positive and therefore $p_g^+ = \max(0, +p_g) = p_g$, which is priced at C_{buy} . Meanwhile, power

cannot be injected from the building to the grid at the same time, and $p_g^- = \max(0, -p_g) = 0$. On the contrary, when power is supplied from the building to the grid, p_g is negative and p_g^- takes its absolute value. This represents an electricity bill reduction of $C_{sell} p_g$.

For visualization purposes, the presented formulation of the problem is not explicit and differs from its implementation. In fact, several nonlinearities are present, such as $\max()$ functions in the constraints and the inverse function in the boiler's model ($T[h+1] = \dots + B \frac{1}{T[h]}$). This challenges MPC stability theory and the accuracy of the numerical solution.

Because linear MPC gives a faster response and is preferred over nonlinear MPC, the algorithm implementation can be made linear with a series of transformations and approximations. For a linear formulation, $\max()$ functions can simply be transformed into inequality constraints accompanied of a $\min()$ function, that can now be introduced in the objective function (minimization problem). Regarding the inverse function, one possible approach is to approximate such a function by a combination of its first-order Taylor expansion, or tangents, which are linear functions. These processes as well as the explicitly linear MPC formulation can be found in Appendix A.

Limitations

The MPC formulation presented above has five optimization variables, namely boiler temperatures, powers and grid power. However, its linear formulation introduces three more variables, one for each boiler and one for ensuring that grid power is not positive and negative at the same time. More importantly, it add to the problem a multitude of additional constraints (see Appendix A). This could have an impact on the fast responsiveness needed to implement MPC, in which case a more advanced embedded system than those required for previous strategies would be needed.

An additional limitation is the need for forecasts, which depending on the accuracy needed could be tenacious or costly to integrate. For instance, an accurate forecast of building's power demand and heat from hot water usage could require a prior period of data acquisition and the training of a model able to associate a certain time of the day, week, and year, to a certain consumption. PV production, which is solely affected by weather and not human activities, is generally easier to predict. Although computationally expensive, it is possible to subscribe to solar irradiation forecasts made by third parties. However, the overall level of accuracy will also depend on the amount of sophistication added. For instance, all-sky cameras could be installed to predict short term (1 to 5 minutes) irradiation variations caused by clouds.

3.4 Strategy 4: MPC of battery and boilers for cost optimization

In strategy 2, the integration of a battery was intended to increase the building's self-consumption when boilers' flexibility was not enough to absorb the totality of surplus power. By installing a small battery, the idea was to use it as a back-up and charge it only during peak production hours.

As a battery can act as a flexible load but also as a flexible generator, implementing MPC enhances its energy management capabilities. When optimizing over a certain horizon, a battery will be incentivized to get charged during low prices and discharged during peak prices. Although doing arbitrage was not the initial intention of installing a battery and may accelerate battery's degradation, an MPC type EMS would make use of that trick to minimize costs even further.

MPC formulation

The objective function remains the same, and battery's power is added to the power balance constraint. Furthermore, battery's model is added as well as its capacity and power limits. For each control time-step h , the boiler and battery commands will be the solution of the following optimization problem:

$$\begin{aligned}
& \min_{\mathbf{u}_B, \mathbf{T}_B, u_{bat}, x_{bat}} \sum_{h=t}^{t+H-1} C_{buy}[h] \max(0, p_g[h]) - C_{sell}[h] \max(0, -p_g[h]) \\
& s.t. \\
& \quad p_g[h] + \hat{p}_x[h] + u_{B1}[h] + u_{B2}[h] + u_{bat}[h] = 0 \\
& \quad x_{bat}[h+1] = x_{bat}[h] + u_{bat}[h]\Delta t \\
& \quad \underline{C}_{bat} \leq x_{bat}[h] \leq \overline{C}_{bat} \\
& \quad \overline{P}_{bat}^{ch} \leq u_{bat}[h] \leq \overline{P}_{bat}^{disch} \\
& \text{for } k = 1, 2 : \\
& \quad T_{B,k}[h+1] = T_{B,k}[h] - A u_{B,k}[h] + B \frac{\hat{E}_{B,k}[h]}{T_{B,k}[h]} - C \hat{E}_{B,k}[h] \\
& \quad \overline{P}_{B,k} \leq u_{B,k}[h] \leq 0 \\
& \quad \underline{T}_{B,k} \leq T_{B,k}[h] \leq \overline{T}_{B,k}
\end{aligned}$$

Limitations

Compared to previous strategy, controlling a battery with MPC does not require additional features except a little extra computing time. In fact, two more variables as well as an additional constraint need to be accounted by the optimization problem.

Furthermore, depending on electricity prices and PV production, such a strategy may force the battery to do several charge/discharge cycles per day, which would heavily impact its lifetime.

4 Implementation and Simulation conditions

4.1 Software architecture

To analyse the feasibility and behaviour of the proposed algorithms, a modular simulation environment representing each of the entities participating in the EMS has been built. It is composed of a central controller able to store and handle all data measurements communicated by the building units. On their side, the different entities run independently, updating their state and always responsive to the controller's command. All together, they model both the building's energy system and the implemented EMS. The architecture schematic is presented in Figure 5. Depending on the 'Strategy' selected, the simulation will instantiate the corresponding units and let the controller know which energy management algorithm to use.

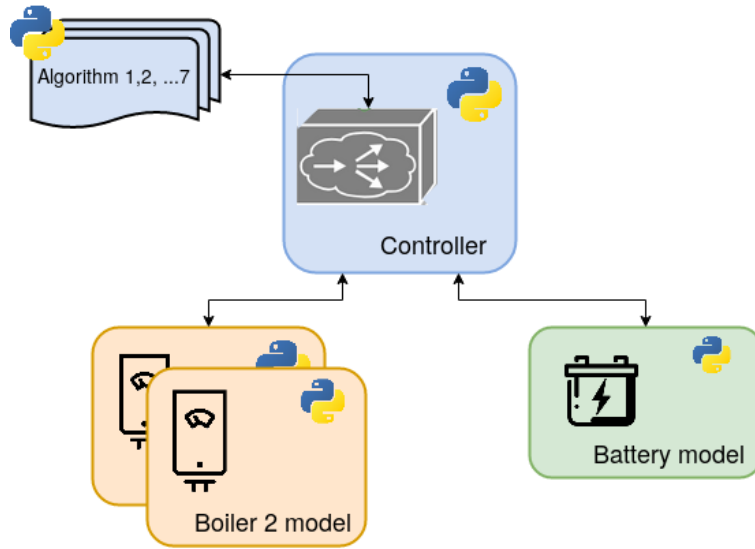


Figure 5: Modular simulation environment communicating via MQTT. All modules are implemented with Python.

Battery and Boilers are represented by Python processes that have their own communication interface with the Controller. For instance, the instantiated battery model contains all its relative information (SoC limits, rated power, etc.) as well as the physical model describing the evolution of its state-of-charge. The model is updated at the process particular frequency, which is independent of the control period but remains the same for all entities.

As the central part of the simulation, the Controller has multiple communication channels, one with each of the entities' models. It is represented by a Python process as well, and by taking the last measurements received, it computes the adequate control actions according to the selected "Strategy". The outputs or commands are communicated back to the entities, which will update their power supply or demand. When an strategy based on optimization is selected, the Controller's MPC algorithm uses *linprog()* function from Python's library *Scipy* to set and solve the linear programming problem.

The communication layer is ensured by MQTT, a publish-subscribe network protocol that transports messages between the devices. When a device publishes a message with a certain topic, devices having subscribed to that topic will receive the message. A Python implementation of MQTT, Paho-MQTT, is used for this framework.

The simulation framework allows the user to select the control strategy as well as parameters such as the simulation horizon, the control period, the updating period for entity models and for MPC approaches, the weight given to the disturbances.

4.2 Building case and simulation characteristics

The comparison of the multiple energy management strategies requires uniform simulation conditions. For that, a building case is set based on real data from consumption and PV production of a residential building in Switzerland, equipped with 72 kWp PV system. The rest of its characteristics, such as boilers parameters, energy of hot water consumed as well as the pricing structure are created for the simulation.

Building

For the 24-hours simulation, a day in March is picked. The building power state at PCC, from which we assume boiler's power supply is not considered, is presented in Figure 6. When positive, surplus supply can go to boilers or the grid. When negative, demand has to be covered by the battery (if any) or the grid.

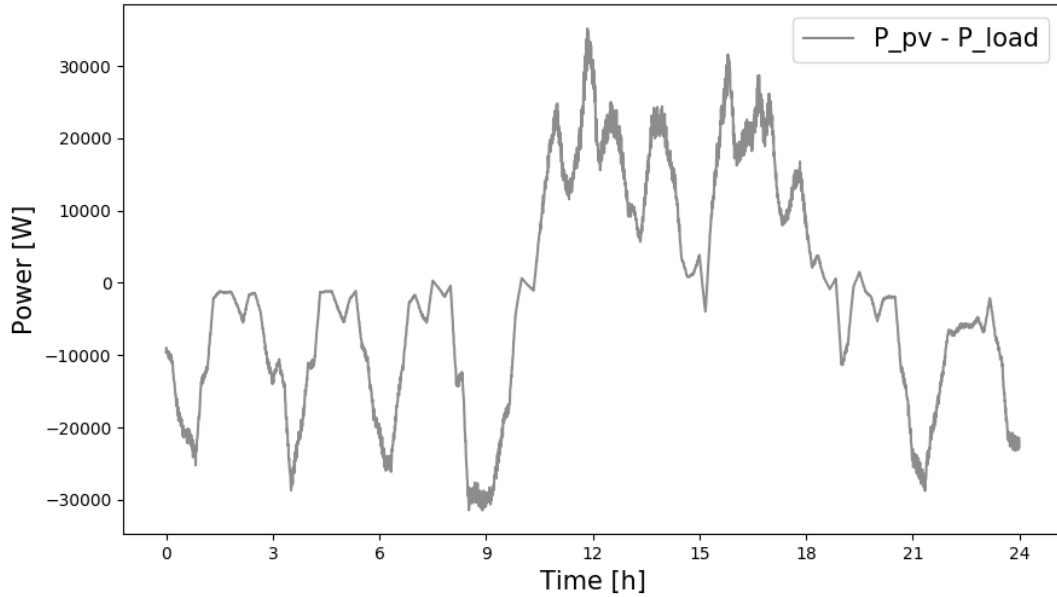


Figure 6: Building's power at PCC (excluding boiler's power) during the 24 hours simulation time.

The energy demanded to the boilers in form of hot water consumption is presented in Figure 7. It has been modelled ensuring that even at peak hot water consumption, boilers' power supply is enough to keep their temperature above lower limits.

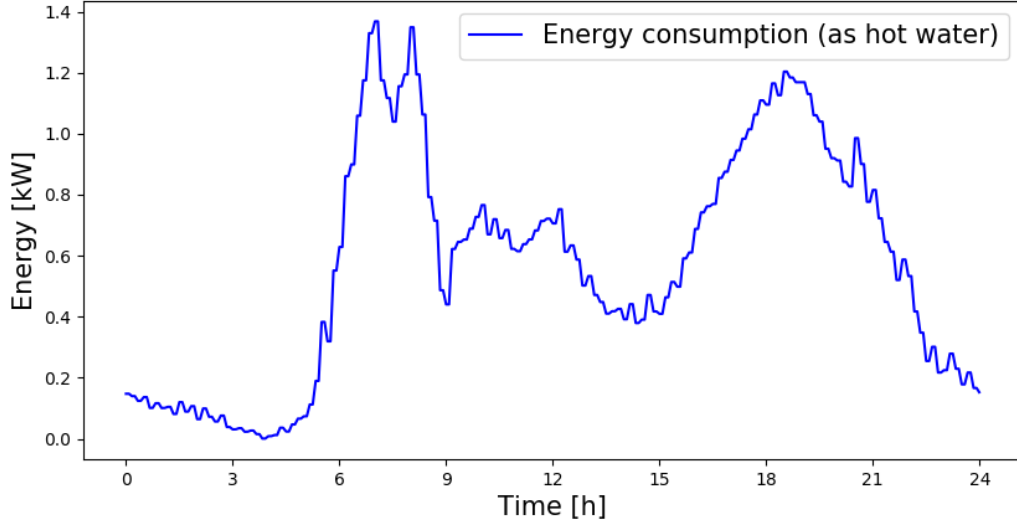


Figure 7: Energy consumed in form of hot water during the 24 hour simulation time.

Controllable entities

Two 800-litres capacity boilers are modelled by Equation 5. A 5 kWh battery is modelled by Equation 2. Both models have an update period of 30 seconds and Tables 1 and 2 present their parameters. For fair comparison between different strategies, the temperature reference for hysteresis control of boilers T_{Δ} is set close to 0.

Appliance	Rated power [kW]	T bounds [°C]	T_{Δ} [°C]	C_B [$\frac{Wh}{^{\circ}C}$]	T_{inc} [°C]	Model period [s]
Boiler 1	-7.6	[40 ; 50]	0.1	927.4	20 °C	30
Boiler 2	-7.6	[30 ; 60]	0.1	927.4	20 °C	30

Table 1: Boilers' specifications.

Appliance	Charging power [kW]	Discharging power [kW]	SoC limits [kWh]	Model period [s]
Battery	-5	5	[0.2 ; 5]	30

Table 2: Battery specifications.

EMS parameters

Considerably higher than the models update period (30 seconds), the EMS control period is set to 300 seconds (5 minutes). Simulation length is 24 hours, and for MPC strategies, the optimization horizon is set to 12 hours to reduce the computing time of control commands.

Disturbances

PCC power and hot-water consumption are the two non-controllable inputs of the EMS. Their forecast is therefore needed for MPC. From PCC power forecast, real values are set randomly so that they don't deviate more than 10% from the prediction. Although not necessarily realistic, it can be seen in Figure ?? how disturbances tend to be bigger (in absolute terms) at positive and negative peaks.

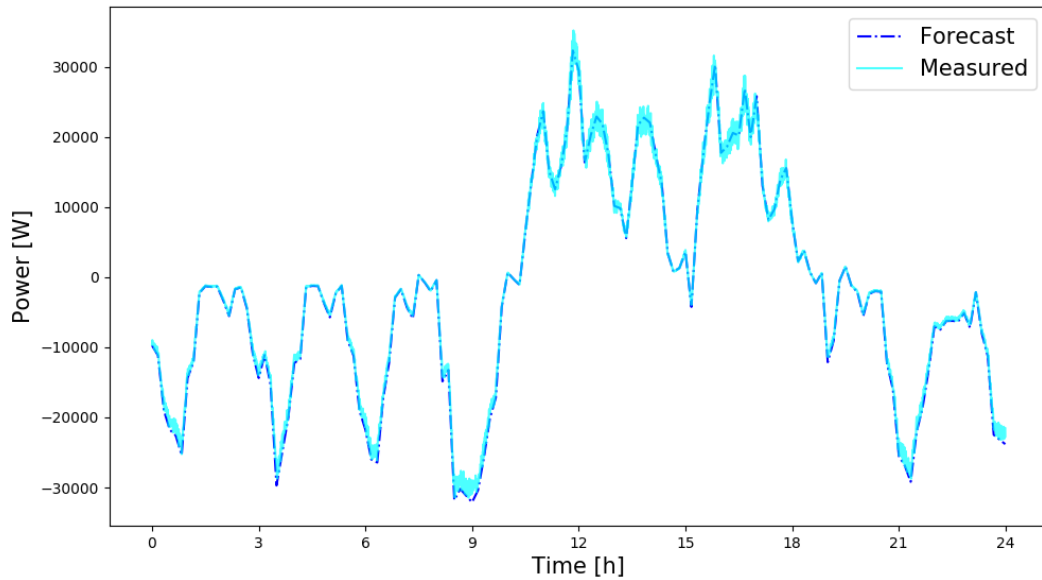


Figure 8: Simulated power at PCC against forecasted profile.

For hot water consumption, disturbances are created manually (see Figure 10).

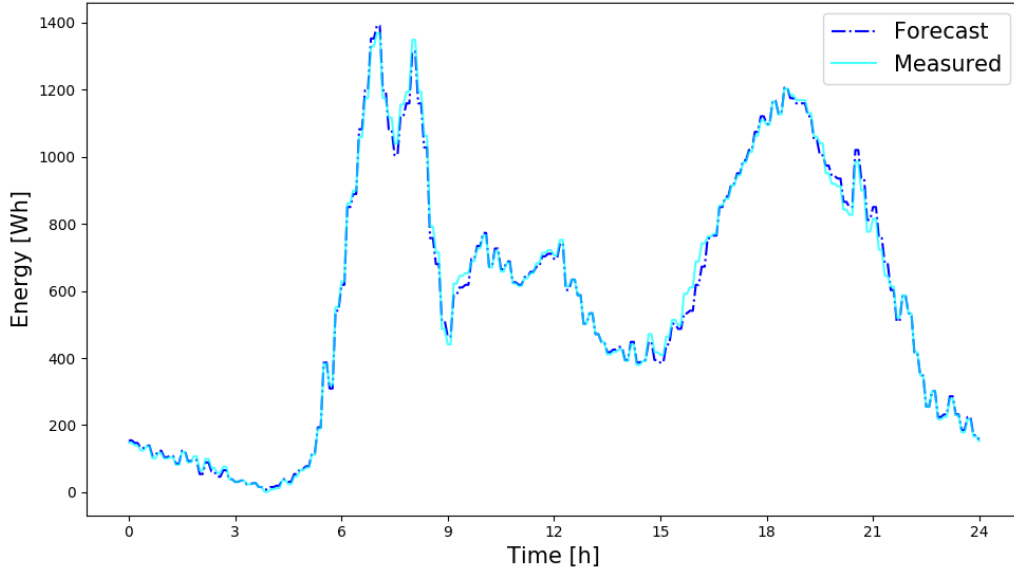


Figure 9: Simulated building's energy consumption against forecasted profile.

Pricing structure

A Time-of-Use (TOU) rate is used, where between 6AM to 10PM, during partial peak demand, cost is higher at 0.24 CHF/kWh. During off-peak, a rate of 0.15 CHF/kWh is charged to use electricity from the grid. This pricing mechanism is particularly used in hot countries, where power demand is highly influence by cooling ventilation and air conditioning. Regarding the Feed-in-Tariff, the building gets 0.08 CHF for each kWh supplied to the grid.

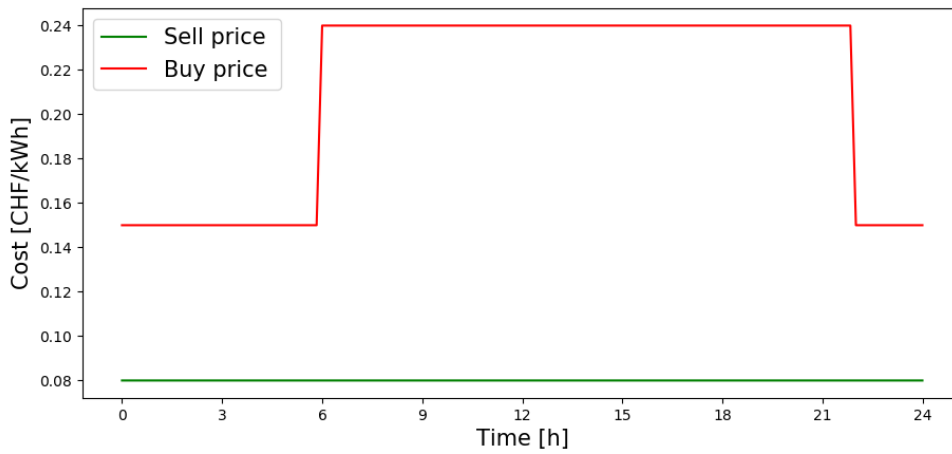


Figure 10: Pricing structure used during the 24 hour simulation time. Price for consuming (red) from the grid follows a TOU rate, and price for supplying the grid (green) is subjected to a constant Feed-in-Tariff.

5 Results

Baseline scenario simulation

Figure 11 presents simulation results for the baseline scenario, where an Energy Management System has not been deployed yet. In the top, the evolution of boilers temperatures and powers can be seen. Below, to serve as reference, the external conditions such as grid tariffs and the total amount of energy demanded to boilers are presented in the sub-figure below. It can be seen that boilers supply is independent of those conditions and that temperatures stay constant around a certain state \underline{T}_B .

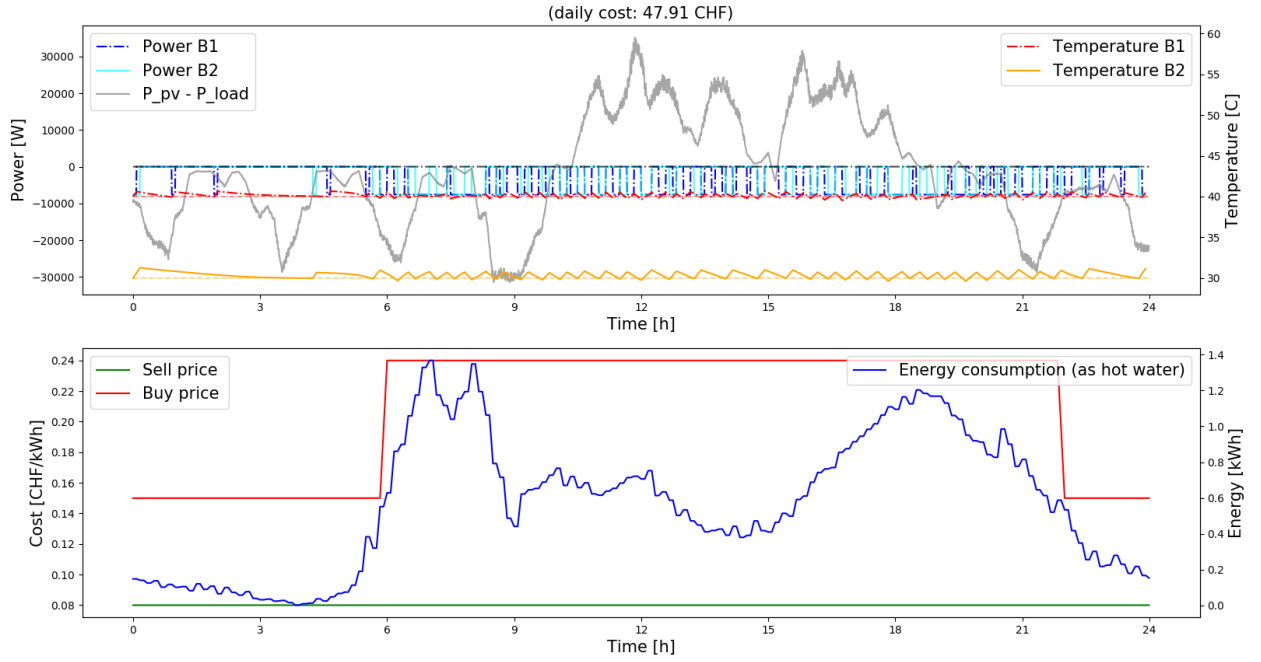


Figure 11: *Baseline scenario*: building's power fluctuations (left y-axis) and evolution of boiler's temperature (right y-axis) when no control strategy is implemented. For reference, bottom graph presents simulation's external conditions.

Because the control period is 5 minutes, temperatures use to go slightly below the minimum temperature for a short while when hot water consumption is high. On the other side, because the supplied power is always the maximum rated power, the temperature often overshoots over $\underline{T}_B + T_\Delta$ when such a command is given to the boilers during 5 minutes.

The cost of the simulated 24 hours is of 47.91 CHF, which is taken as a reference for comparing the coming control strategies.

Strategy 1: rule-based control of boilers

Strategy 1 consists in making use of boilers flexibility to power them above their minimal temperature T_B with the use of surplus power. For reference, the upper and lower temperature bounds marking that flexibility are highlighted in Figure 12 by dotted lines. As expected, it can be seen that during times of high PV generation, boilers temperatures leave their lower bound to attain higher values.

Interestingly, one of the limitations described in strategy 1 presentation can be observed. After $t = 16h$, when PV production increases again, boiler B1 supply is reduced even if surplus power is abundant and the boiler entity has not reached its upper temperature bound. According to the simplistic boiler model taken into account by the controller (which does not consider hot water consumption), the thermo-electric load has already reached its desired state, and less power is needed to keep it at such state. This mismatch between boiler true simulated model and control model has a consequence on the EMS self-consumption capabilities.

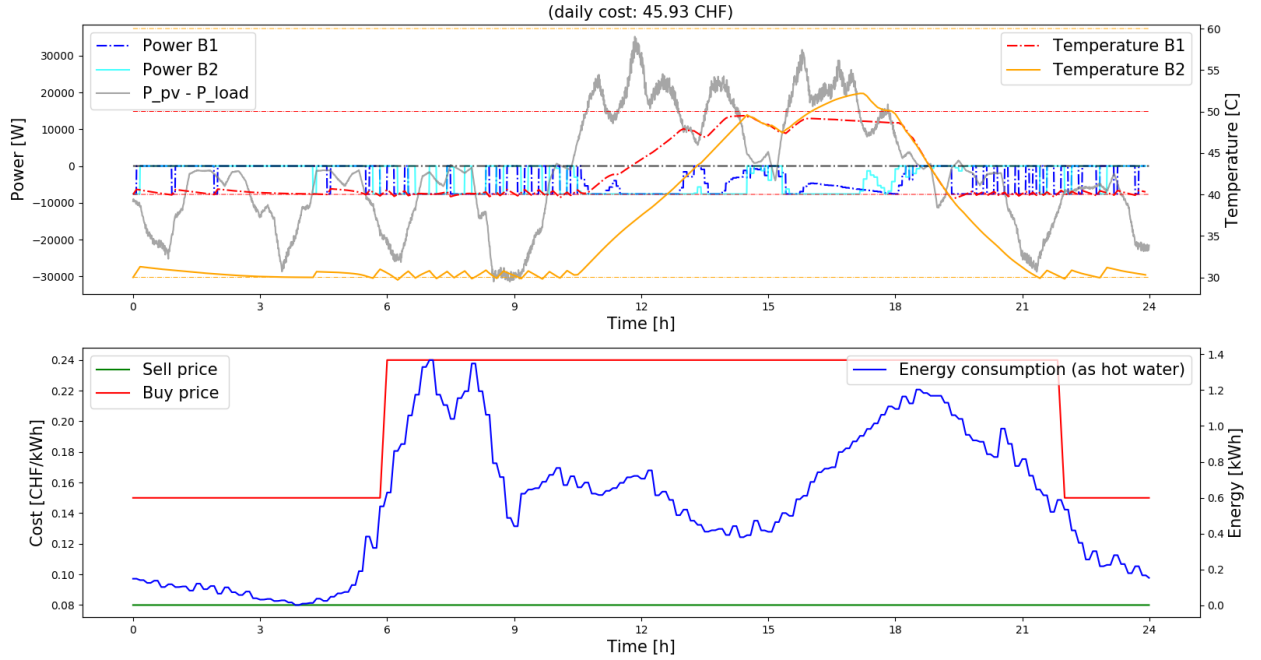


Figure 12: *Strategy 1*: building's power fluctuations (left y-axis) and evolution of boiler's temperature (right y-axis) as a result of a rule-based control of boilers. At times of high PV production, surplus power is used to power boilers. For reference, bottom graph presents simulation's external conditions.

As more electricity is self-consumed, the demand for grid's electricity is reduced. This translates in a 24-hour cost of 45.93 CHF, or a reduction of 1.98 CHF (4.13%) by implementing strategy 1.

Strategy 2: considering a battery for rule-based control

The installation of a battery system is intended to enhance self-consumption. It was visible that with previous strategy, during times of high PV generation, boilers were being powered at their maximal rated power most of the time. However, surplus power was still positive and therefore sold the grid at a lower price than the cost of buying later. At a particular time, power intake of boiler B1 was also limited by its temperature limits.

Figure 13 shows how the newly integrated 5kWh battery is precisely charged at such moments, when surplus power is at its peaks and exceeds boilers supply capacities. By looking at the State-of-Charge (SoC) evolution, one can see that the battery does not take long to reach its full capacity and is therefore not able to absorb all surplus. Whenever power demand surpasses supply again, the battery is immediately discharged, covering only a small portion of the building's consumption.

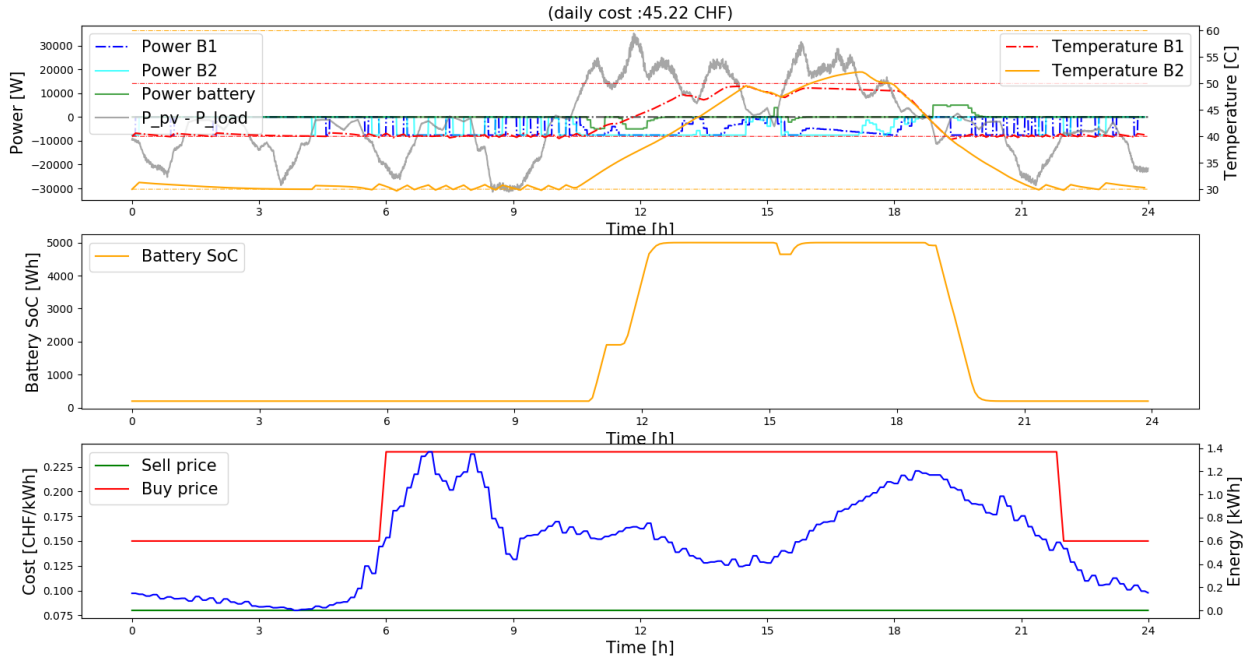


Figure 13: *Strategy 2*: Building's power fluctuations (left y-axis) and evolution of boiler's temperature (right y-axis) as a result of adding a battery and applying rule-based control for self-consumption. Middle graph illustrates the evolution of the battery State-of-Charge. For reference, bottom graph presents simulation's external conditions.

As expected, the contribution of the battery is minimal if we compare it with the building net power peak values. However, as back-up source of flexibility, it is still capable of enhancing self-consumption and reduce costs. With a total cost of 45.22 CHF, strategy 2 allows to reduce the simulated 24-hour bill by a total of 2.69 CHF (5.61%). Compared to strategy 1 where a similar rule-based algorithm

is only applied to boilers, the reduction is of 0.71 CHF (1.54%).

Strategy 3: Applying MPC to boilers

Figure 14 presents the daily evolution of boiler states subjected to an MPC strategy. It is clearly visible how the cost of buying is taken into account by the EMS, which powers boiler until the moment when price increases ($t = 6h$), at which point both temperatures have reached their upper value. In the case of boiler B1, this supply allows it to withstand without being powered during high-price period, until surplus power arises. Regarding boiler B2, it may seem that its supply has been excessive during the low-price period. In fact, it reaches surplus time with a higher temperature than the minimal required $T_{B2} = 30^\circ\text{C}$. This behaviour was however planned by MPC, which anticipated the hot water consumption peak of noon and left some extra energy in B2. By doing this, MPC ensured that the boiler could remain in suitable operating conditions without the need to be powered by high-priced grid power.

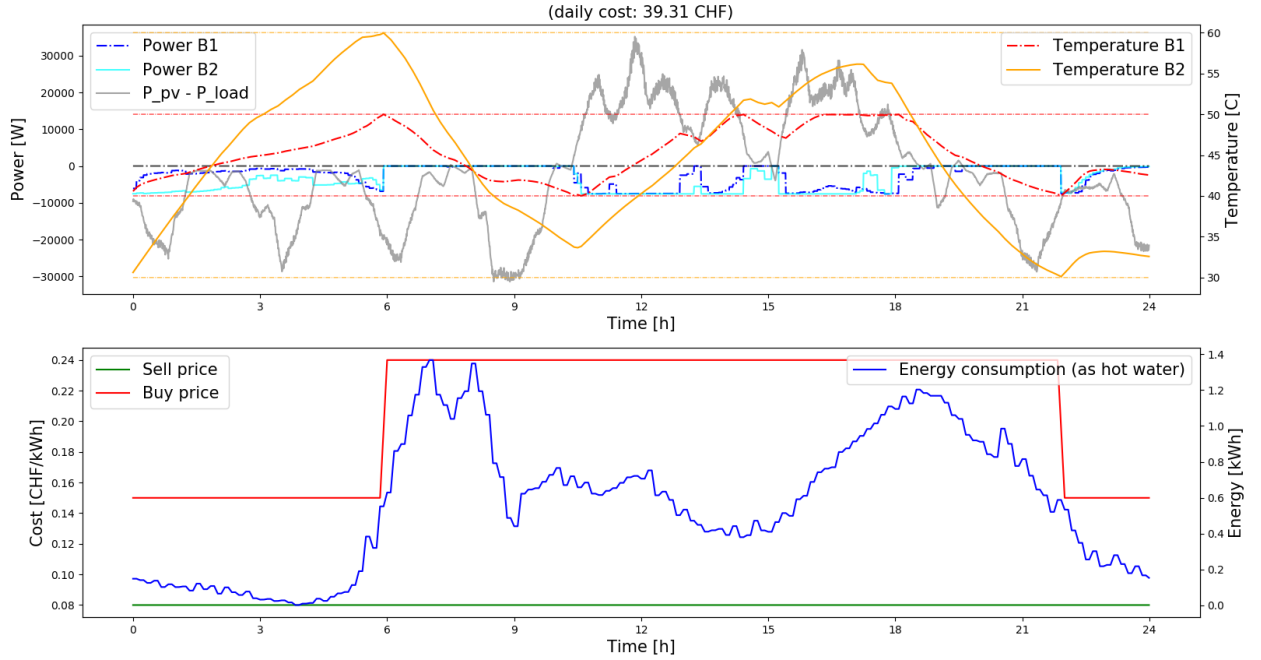


Figure 14: *Strategy 3*: building's power fluctuations (left y-axis) and evolution of boiler's temperature (right y-axis) as a result of MPC of boilers. For reference, bottom graph presents simulation's external conditions

It is also interesting to see that the implementation of MPC brings more accuracy to the control action. The algorithm incorporates a more detailed boiler model which takes into account the energy demanded by the building in the form of hot water (see model in Equation 5). At the times where strategy 1 was not able to bring boiler B1 to its upper limit (at around $t = 17h$), MPC does it

accurately.

The implementation of MPC brings the daily simulated cost to 39.31 CHF, making the higher reduction (5.91 CHF or 13.07%) when one takes the previous strategy as a reference. Compared to the baseline scenario, the cost is reduced by 8.6 CHF (18.0%).

Strategy 4: MPC of battery and boilers

Results of strategy 4 (see Figure 15) can be first compared to strategy 2, where the same battery was controlled with a rule-based algorithm. In the MPC case, the charging happens during low-priced period. After that, it is progressively discharged until depletion. During high PV generation time, the battery is charged with surplus and discharged once again until the cost of buying is decreases. At this point, the battery starts being charged a fourth time preparing for the next day and charges.

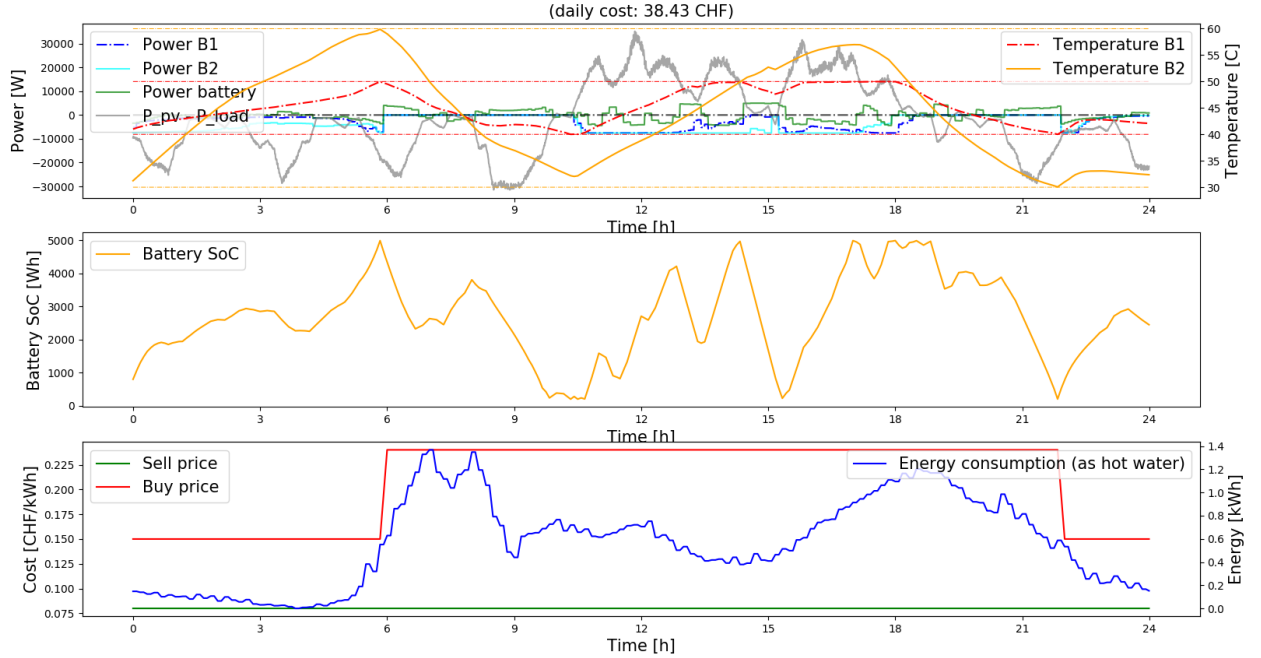


Figure 15: *Strategy 4*: building's power fluctuations (left y-axis) and evolution of boiler's temperature (right y-axis) as a result of applying MPC to battery and boilers. For reference, bottom graph presents simulation's external conditions

However, a non-desirable behaviour can be found: the battery SoC fluctuates more than it should. For instance, at times of constant prices, when there is no incentives to do so, the battery charges and discharges, as if it was a path for electricity to go from the grid to boilers. This happens right after $t = 3h$, where instead of powering boilers with grid's power, the battery is used. Also at time

of surplus, the battery is intermittently charged and discharged to give additional surplus to boilers. This unintended behaviour occurs because the cost of using the battery is zero and could be partially solved by simply setting a charging and discharging efficiencies lower than 100%.

With this combination of MPC strategy and battery integration, costs are reduced by 0.88 CHF (2.24%) compared to an only-boiler MPC strategy, and by 6.79 CHF (15.02%) compared to rule-based control of battery.

Table 4 summarizes all cost reductions achieved by implementing one strategy or another.

	Strategy 1 45.93 CHF	Strategy 2 45.22 CHF	Strategy 3 39.31 CHF	Strategy 4 38.43 CHF
Baseline	4.13%	5.61%	18.0%	19.79%
Strategy 1	×	1.54%	14.41%	16.33%
Strategy 2	×	×	13.07%	15.02%
Strategy 3	×	×	×	2.24%

Table 3: Summary of cost reduction achieved by implementing one strategy over the other. As reference, cost of simulated baseline scenario is 47.91 CHF. *Interpretation to be done by columns (i.e. the implementation of strategy 1 (column) on top of baseline (line) reduces costs by 4.13%)*

	Strategy 1 40.02 CHF	Strategy 2 39.49 CHF	Strategy 3 35.55 CHF	Strategy 4 35.05 CHF
Baseline	2.65%	3.94%	13.52%	14.74%
Strategy 1	×	1.32%	11.17%	12.42%
Strategy 2	×	×	9.98%	11.24%
Strategy 3	×	×	×	1.41%

Table 4: Summary of cost reduction for simulations ran with a different Time-of-Use tariff (0.2 instead of 0.24 CHF/kWh for high buy price). As reference, cost of simulated baseline scenario with this pricing structure is 41.11 CHF. *Interpretation to be done by columns (i.e. the implementation of strategy 1 (column) on top of baseline (line) reduces costs by 4.13%)*

6 Discussion

As presented in Table 4, strategy 4 outperforms the rest in terms of cost reduction. As expected, such an EMS is capable of capitalizing on both forecast-based optimization and additional flexibility. It requires however a battery, whose costs should be considered too for a fairer comparison.

6.1 Battery integration: a questionable option

Beforehand, the integration of a battery was expected to be significantly more suitable for an MPC type strategy. Instead, cost reductions brought by its incorporation are very similar. In strategy 2, where battery only takes surplus power, savings achieved are of 0.7 CHF/day (with respect to no-battery case). In strategy 4, battery is charged and discharged every time a price variation appears in the horizon, but still achieves a cost reduction of 0.88 CHF/day. Considering the generally recommended *one cycle per day*, and MPC approach for battery control does not seem the most adequate in this particular case. The consequences of that could be an accelerated degradation and a premature end of life.

Nevertheless, in order to address the profitability question, the cost of a battery can still be considered in the myopic strategy. Even if prices can vary considerably according to specifications, an average price of 0.31 CHF/kWh is estimated for competitive companies such as Tesla or LG [7]. Accounting therefore for an average initial investment of 1550 CHF and the cost savings of 0.7 CHF/day, a very rough approximation can be made on the payback time for the battery: 2214 days, or 6 years. With a conservative assumption of a 10 years lifetime (equal to the warranty given by providers mentioned above), strategy 2 would result slightly profitable over strategy 1, in the long run. Considering all the assumptions made, this simplistic analysis must be thread carefully. Moreover, a one-day simulation is used to approximate costs of a 6 year period.

6.2 MPC: confirmed benefits and limitations

Although the battery participates in the savings of strategy 4, the major component of that cost reduction is due to MPC. By looking at cost savings data presented in Table 4, it is explicit that MPC approaches are substantially better for reducing costs than the alternative myopic algorithms.

The benefits of MPC in terms of cost were already expected, but their design was followed by a warning about two relevant limitations. The first one was the need for forecasts, which is often technically challenging or costly. The second, associated to its additional computational costs, was confirmed true during simulations. The linearized MPC formulation for boilers' control presented 7 decision variables as well as 12 constraints. A required tolerance of 10^{-6} was set for the numerical solution. For the reference, simulations were carried on a single HP Pavillon laptop (2017, i7, 16gb RAM). In such conditions and accounting for a 12-hour horizon (144 control intervals), one MPC iteration needed from 80 to 120 seconds to compute. On top of making simulation very long, this behaviour wouldn't be accepted if the same device was used to perform real-time control in a building.

6.3 Study limitations

In the presented study case, the effectiveness of MPC against a myopic approach is pronounced. It is however strengthened by suitable simulation conditions.

For instance, time-dependent electricity tariffs alone are a strong argument to implement MPC. Those rates are not subjected to any sort of disturbances or uncertainties, and are consequently a strong base from which the MPC algorithm can optimize energy flows. In theory, the highest the amplitude of those variations, the more MPC is going to stand out from a myopic algorithm. In the simulated case, the difference between high buy tariff (0.24 *CHF/kWh*) and low buy tariff (0.15 *CHF/kWh*) is significant. Against a myopic algorithm that is blind to such price variations, an MPC approach comes therefore far out ahead.

The other way around, we can expect that the smaller the price gap, the lower the difference of both approaches would be in terms of costs. Brought to an extreme, we could actually anticipate very similar profiles for MPC and rule-based control for self-consumption in a simulation case with a constant buying rate.

Another delicate point are forecasts, which in the simulated case remain very accurate predictions of the actual values (see Figures 8 and 9). In reality, stochastic quantities influenced by human behaviour (building loads and hot water consumption) or weather conditions (PV production) are very hard to accurately predict. In the performed simulations, the sequential optimization process is not challenged by important disturbances that would make it deviate significantly from its optimal path. This makes the overall energy management close to optimal, which may not be the case with less accurate predictions.

Performing a series of simulations with different degrees of disturbances would clarify the efficacy of MPC and lead to a fairer comparison. Furthermore, such analysis would allow to better estimate its advantages over a rule-based strategy in the cases where the accuracies of the available forecasting techniques are known.

7 Conclusion

In a scenario where decreasing PV prices are counterbalanced by a reduction of incentives for PV installations, the benefits of implementing Energy Management Systems in commercial or residential microgrids arise. To further evaluate those benefits, this report presented 4 strategies to control and manage energy flows in a residential building equipped with flexible loads, namely two electric boilers. First, a myopic rule-based algorithm for boilers' control was proposed to increase PV self-consumption. Second, an MPC approach capable of optimizing costs based on building future state predictions was presented. In parallel, two additional strategies consisted in integrating a battery system to both myopic and MPC approaches, with the intention to enhance self-consumption in the first case and reduce costs in the second.

To test the functioning of the different control algorithms, a modular framework was developed with Python. Enabled by a communication layer, it allowed to simulate the behaviour of both the controller and flexible loads, each being an independent process, and to accordingly compute the electricity costs of the performed simulation.

Simulations were conducted using PV generation and load consumption field data from a residential building. On the grid side, a Time-of-Use pricing scheme defined by a higher rate from 6AM to 10PM was used. Results successfully showed that each of the proposed energy management strategies progressively lowered electricity costs. In particular, the incorporation of a basic EMS based on a rule-based logic reduced the building electricity bill by 4.13%. Better cost reduction capabilities were presented by MPC, which significantly reduced bills by 18%. In both myopic and MPC approaches, the integration of a 5kWh battery reduced costs by 1.54% and 2.24% respectively. From both strategies, only the rule-based control appropriately handled the battery as back-up source of flexibility. Accounting for a standard battery price, savings made the case for an estimated investment payback time of 6 years. On the other side, justified by an excessive number of daily cycles, the presented MPC approach was not recommended for a favorable battery operation.

Particularly for MPC, positive results were subjected to various limitations. Because simulated forecasts remained considerably accurate, successful cost optimization did not get challenged by big disturbances. Furthermore, nonlinearities in the formulation made the problem computationally costly for a mid-range personal computer, setting doubts for the case of a real-time implementation.

Finally, the simulated case gave an example of the main parameters to take into account when designing an appropriate EMS. At the beginning, the limited amount of flexible loads did not particularly advocate for the implementation of MPC, which requires forecasts and has higher demands in terms of hardware. However, the variability of electricity prices showed to be a strong argument for MPC implementation, which proved to be a considerably better approach to reduce energy costs. Moving towards a liberalized scenario where retail electricity prices will be also influenced by supply and demand, the benefits of MPC can quickly overcome its limitations.

A Linearization of MPC formulation

This section illustrates the linearization process of the following nonlinear MPC fomulation, presented in section 3.3 for boilers control:

$$\begin{aligned}
& \min_{\mathbf{u}_B, \mathbf{T}_B, p_g} \sum_{h=t}^{t+H-1} C_{buy}[h] \max(0, +p_g[h]) - C_{sell}[h] \max(0, -p_g[h]) \\
& s.t. \\
& p_g[h] + \hat{p}_x[h] + u_{B1}[h] + u_{B2}[h] = 0 \\
& \text{for } k = 1, 2 : \\
& T_{B,k}[h+1] = T_{B,k}[h] - A u_{B,k}[h] + B \frac{\hat{E}_{B,k}[h]}{T_{B,k}[h]} - C \hat{E}_{B,k}[h] \\
& \bar{P}_{B,k} \leq u_{B,k}[h] \leq 0 \\
& \underline{T}_{B,k} \leq T_{B,k}[h] \leq \bar{T}_{B,k}
\end{aligned}$$

1) Handling the $\max()$ function

The *max-removal* transformation is a standard problem re-writing rule that removes a *max* term from the objective function.

The instance

$$\max(0, -p_g) \tag{9}$$

can be transformed in

$$\min \phi \quad s.t. \quad \phi \geq 0 \quad \text{and} \quad \phi \geq -p_g \tag{10}$$

The solution of problem 10 is the smallest upper-bound, 0 or $-p_g$, which is in fact the highest value of both (solution of problem 9). The objective function of the recently presented MPC can be transformed into the following:

$$\begin{aligned}
& \min_{\hat{\mathbf{u}}_B, \mathbf{T}_B, p_g, \phi} \sum_{h=t}^{t+H-1} \phi \\
& s.t. \\
& \phi \geq C_{buy}[h] p_g[h] \\
& \phi \geq C_{sell}[h] p_g[h]
\end{aligned}$$

2) Handling the inverse function

The term $\frac{1}{T[h]}$ is approximated by a combination of its tangents at several points in the feasible region of T (40 °C to 50 °C for instance). This combination of tangents is denominated as $\{tan_{40}, tan_{42}, \dots, tan_{50}\}$. In the temperature bounds, $f(x) = \frac{1}{x}$ is a convex function, which means that at any temperature T^* , $\frac{1}{T^*}$ will be greater or equal to any of the points given by applying T^* to each of the tangents in $\{tan_{40}, tan_{42}, \dots, tan_{50}\}$. Hence, the tangent that will minimize the approximation will be, at a certain point T^* , obtained by $\max[\{tan_{40}, tan_{42}, \dots, tan_{50}\}(T^*)]$.

As with the *max-removal* transformation, we can transform the *max* into a *min* and inequality constraints. Such *min* is added to the objective function, as a penalty, with a certain weight w . The final linear problem is written as follows:

$$\begin{aligned}
& \min_{\mathbf{u}_B, \mathbf{T}_B, p_g, \phi, \epsilon_B} \sum_{h=t}^{t+H-1} \phi + w (\epsilon_{B1} + \epsilon_{B2}) \\
& s.t. \\
& \quad p_g[h] + \hat{p}_x[h] + u_{B1}[h] + u_{B2}[h] = 0 \\
& \quad \phi \geq C_{buy}[h] p_g[h] \\
& \quad \phi \geq C_{sell}[h] p_g[h] \\
& \text{for } k = 1, 2 \\
& \quad T_{B,k}[h+1] = T_{B,k}[h] - A u_{B,k}[h] + B \hat{E}_{B,k}[h] \epsilon_{B,k} - C \hat{E}_{B,k}[h] \\
& \quad \epsilon_{B,k} \geq \tan_i\left(\frac{1}{T_{B,k}[h]}\right) \quad \text{for } i \in [\underline{T}_{B,k}; \overline{T}_{B,k}] \\
& \quad \overline{P}_{B,k} \leq u_{B,k}[h] \leq 0 \\
& \quad \underline{T}_{B,k}[h+1] \leq T_{B,k}[h] \leq \overline{T}_{B,k}[h+1]
\end{aligned}$$

For the implementation, lowering the weight w to 0.2 gives enough priority to the cost term ϕ . Also, choosing 5 points in the temperature range to obtain 5 tangents for each boiler gives a good enough optimization and a faster response, as each of them is an extra constraint for the MPC.

References

- [1] Marco Antonelli and Umberto Desideri. Do feed-in tariffs drive PV cost or viceversa? *Applied Energy*, 135:721–729, December 2014.
- [2] Giovanni Brusco, Alessandro Burgio, Daniele Menniti, Anna Pinnarelli, and Nicola Sorrentino. The economic viability of a feed-in tariff scheme that solely rewards self-consumption to promote the use of integrated photovoltaic battery systems. *Applied Energy*, 183:1075–1085, December 2016.
- [3] Cherrelle Eid, Elta Koliou, Mercedes Valles, Javier Reneses, and Rudi Hakvoort. Time-based pricing and electricity demand response: Existing barriers and next steps. *Utilities Policy*, 40:15–25, June 2016.
- [4] International Energy Agency (IEA). “Solar Energy: Mapping the road ahead”, October 2019, www.iea.org, Accessed: 2020-01-04.
- [5] M. Karimi, H. Mokhlis, K. Naidu, S. Uddin, and A.H.A. Bakar. Photovoltaic penetration issues and impacts in distribution network – a review. *Renewable and Sustainable Energy Reviews*, 53:594–605, January 2016.
- [6] Office of Gas and Electricity Markets (ofgem). “Feed-In Tariff (FIT) rates”, April 05 2019, <https://www.ofgem.gov.uk/environmental-programmes/fit/fit-tariff-rates>, Accessed: 2020-01-04.
- [7] Solar Quotes. “Solar Battery Storage Comparison Table”, 24th Dec 2019, <https://www.solarquotes.com.au/battery-storage/comparison-table/>, Accessed: 2020-01-05.